(1)

AD_____

Grant Number DAMD17-96-1-6129

TITLE: Metastatic Tumor Cell Behavior in Situ

PRINCIPAL INVESTIGATOR: John Condeelis, Ph.D.

CONTRACTING ORGANIZATION: Albert Einstein College of Medicine
Bronx, New York 10461

REPORT DATE: October 1998

TYPE OF REPORT: Final

PREPARED FOR: U.S. Army Medical Research and Materiel Command
Fort Detrick, Maryland 21702-5012

(2)

REPORT DOCUMENTATION PAGE

Form Approved
OMB No. 0704-0188

Condeelis, John S.

1. AGENCY USE ONLY *(Leave blank)*	2. REPORT DATE	3. REPORT TYPE AND DATES COVERED
	October 1998	Final (15 Sep 96 - 14 Sep 98)

4. TITLE AND SUBTITLE
Metastatic Tumor Cell Behavior in Situ

5. FUNDING NUMBERS
DAMD17-96-1-6129

6. AUTHOR(S)
John Condeelis, Ph.D.

7. PERFORMING ORGANIZATION NAME(S) AND ADDRESS(ES)
Albert Einstein College of Medicine
Bronx, NY 10461

8. PERFORMING ORGANIZATION REPORT NUMBER

9. SPONSORING/MONITORING AGENCY NAME(S) AND ADDRESS(ES)
Commander
U.S. Army Medical Research and Materiel Command
Fort Detrick, Frederick, Maryland 21702-5012

10. SPONSORING/MONITORING AGENCY REPORT NUMBER

19990407 110

11. SUPPLEMENTARY NOTES

12a. DISTRIBUTION / AVAILABILITY STATEMENT
Approved for public release; distribution unlimited

12b. DISTRIBUTION CODE

13. ABSTRACT *(Maximum 200*

During metastasis from a primary tumor, cell motility is believed to be important for dissemination of tumor cells from the primary tumor, and the steps called intravasation and extravasation. Proof that the active motility of tumor cells is a key component in metastasis would be a major advance. An understanding of the mechanisms of cell motility in metastatic tumor cells *in vivo*, in particular, would be important for a more rational system of diagnosis and treatment of metastatic cancers. We have developed a new method for imaging tumor cells in live animals and have identified subpopulations of moving cells within primary breast tumors. It is clear that metastatic tumor cells are actively motile as they disseminate from the primary site. This information supports the three-step hypothesis of metastasis which proposes that motility is necessary for a cell to metastasize. This model will be useful in describing and tracking the behavior and interactions of these metastatic tumor cells *in vivo*. In addition, it represents an opportunity to reliably procure pure populations of motile tumor cells *in vivo* under direct observation.

14. SUBJECT TERMS	15. NUMBER OF PAGES
Breast Cancer	17
	16. PRICE CODE

17. SECURITY CLASSIFICATION OF REPORT	18. SECURITY CLASSIFICATION OF THIS PAGE	19. SECURITY CLASSIFICATION OF ABSTRACT	20. LIMITATION OF ABSTRACT
Unclassified	Unclassified	Unclassified	Unlimited

(3)

FOREWORD

Opinions, interpretations, conclusions and recommendations are those of the author and are not necessarily endorsed by the U.S. Army.

✓ Where copyrighted material is quoted, permission has been obtained to use such material.

✓ Where material from documents designated for limited distribution is quoted, permission has been obtained to use the material.

✓ Citations of commercial organizations and trade names in this report do not constitute an official Department of Army endorsement or approval of the products or services of these organizations.

✓ In conducting research using animals, the investigator(s) adhered to the "Guide for the Care and Use of Laboratory Animals," prepared by the Committee on Care and use of Laboratory Animals of the Institute of Laboratory Resources, national Research Council (NIH Publication No. 86-23, Revised 1985).

____ For the protection of human subjects, the investigator(s) adhered to policies of applicable Federal Law 45 CFR 46.

✓ In conducting research utilizing recombinant DNA technology, the investigator(s) adhered to current guidelines promulgated by the National Institutes of Health.

✓ In the conduct of research utilizing recombinant DNA, the investigator(s) adhered to the NIH Guidelines for Research Involving Recombinant DNA Molecules.

____ In the conduct of research involving hazardous organisms, the investigator(s) adhered to the CDC-NIH Guide for Biosafety in Microbiological and Biomedical Laboratories.

J Iandelli 10/23/98

PI - Signature Date

(4)

Table of Contents

		Pages
1.	**Table of Contents**	1
2.	**Introduction**	2
3.	**Body**	2-4
4.	**Conclusions**	4
5.	**References**	5
6.	**Appendix**	6

(5)

Introduction

Metastasis represents the major cause of mortality in breast cancer patients. Components of the metastatic process can include growth at the primary site, attraction of new blood vessels to the primary tumor, dissemination of tumor cells in the surrounding connective tissue, intravasation and distribution of tumor cells in the bloodstream or lymphatics, spread to axillary lymph nodes, extravasation across blood vessel walls and into the tissue parenchyma at a secondary site, and growth at the secondary site. These components encompass and rely upon a large number of cellular functions. Cell motility is believed to be important for dissemination of cells from the primary tumor, intravasation and extravasation. Proof that the motility of tumor cells is a key component in metastasis would be a major advance.

We have developed a model that directly examines the motility of non-metastatic and metastatic tumor cells in live primary tumors *in situ.* Non-metastatic and metastatic rat breast cancer cell lines were each prepared to constitutively express green fluorescent protein (GFP). Upon subcutaneous injection of these cells into the mammary fat pad of female Fischer 344 rats, primary and metastatic tumors form that fluoresce when excited with FITC filtered light (1). Animations of metastatic tumor cells moving in live rats were generated by intravital imaging of the primary tumor, i.e. in the live animal under anesthesia, on a laser scanning confocal microscope. With this model, the behavioral phenotype of metastatic and non-metastatic tumor cells can be described and determined. Furthermore, this model can be extended to any type of tumor cell that grows as a primary tumor subcutaneously. It is the first model that allows direct observations of metastasis in an intact orthotopically grown primary tumor while in a live animal.

(6)

Body

Non-metastatic and metastatic tumor cell lines used in these experiments are the MTC and MTLn3 lines, respectively. These cell lines represent a well characterized cell pair which were derived from the same original tumor and which retain their relative metastatic phenotypes after prolonged culture (2, 3). Examination of the behavior of cells in the MTC (non-metastatic) and MTLn3 (metastatic) derived tumors demonstrates significant differences between the two. Non-metastatic tumors are more fibrous and less necrotic. The tumor cells are farther apart due to intervening extracellular matrix and host cells, and the tumor cells are more arborized but not motile (Figure 1). Metastatic tumors are more necrotic and the tumor cells are tightly packed due to less extracellular matrix and fewer intervening host cells. The tumor cells are less arborized and exhibit dramatic motility not seen in non-metastatic tumors (1, 4) (Figure 1).

Cellular locomotion occurring in the metastatic tumors is described here. Metastatic cells moving in the primary tumor often move as groups or streams of cells suggesting a preferred micro-environment for locomotion in vivo. The average instantaneous velocity of cells, from four different metastatic primary tumors, was measured as 3.0 um/min. However, in all of the tumors examined, it was apparent that only a small fraction of primary tumor cells are actively motile during any given imaging interval. For some of these cells, instantaneous velocity values were close to the persistence value indicating a high degree of rectilinear motion reminiscent of chemotaxis.

The velocities of ~3 um/min shown by cells in the primary tumor are higher than velocities exhibited by cells in culture during either random motility (0.45 um/min +/- 0.08, n=8) or highly persistent motility (0.82 um/min +/- 0.19, n=8) observed in a gradient of EGF, which is chemotactic for metastatic adenocarcinoma cells (5). Besides velocity and persistence, additional parameters that one can compute using a DIAS analysis are described elsewhere (6) and shown in the video.

Our model is described in detail in the reprint (ref. 1 and the appendix) supplied and images acquired in live animals can be viewed on our web site www.aecom.yu.edu by clicking on Analytical Imaging Facility and Farina et al in the Bibliography. What follows is a description of the video:

Sequence 1: A mammary adenocarcinoma cell (MTLn3) exhibits chemotactic movement toward a pipette filled with EGF. When the pipette (P) is moved to elude the cell, the cell turns directly towards the pipette without hesitation. The cell diameter is approximately 25 microns. The sequence is repeated. Time scale shown is min:sec.

Sequence 2: Chemotaxis-like persistent locomotion occurs in a population of cells in vivo. Confocal time lapse images in a single optical plane of an intact living tumor prepared by injection of MTLn3 cells into the mammary fat pads of Fisher rats. Two and a half weeks after injection, a tumor forms which can be exposed by relatively non-invasive surgery to remove the overlying cutaneous layer exposing the tumor to the microscope objective. The arrow indicates the position of a blood vessel (non-fluorescent) toward which the cells move with a high degree of persistence. Cells move in a stream. The velocity of movement is approximately 3 microns per minute. This movement is highly rectilinear and is reminiscent of chemotactic movements observed in culture in response to a pipette of EGF and may result from chemotaxis to serum components. The sequence repeats. Scale bar = 50 um. 350x real time.

Sequence 3: When mammary adenocarcinoma cells (MTLn3) are subjected to an increase in the EGF concentration in culture, they undergo cycles of protrusion and retraction. The addition of 5 nM EGF is indicated by the letters EGF. The immediate response of the cells is inhibition of ruffling followed by rapid extension of lamellipods and this appears synchronously in culture. The cells then begin retraction and ruffling. The sequence is repeated. Cell diameter is approximately 25 microns.

Sequence 4: Adenocarcinoma cells in vivo exhibit cycles of protrusion and retraction when in contact with a blood vessel. Split screen demonstration of the behavior of a cell in a live intact primary tumor when it has made direct contact with the surface of a blood vessel. On the left is the raw data. The black background is the surface of a large vessel. The cell goes through a series of protrusion and retraction cycles repeatedly as it extends and retracts in position without net locomotion. The right-hand side of the split screen shows the DIAS difference picture, where the protrusions are indicated in green and the retractions in red. The star at the center of the cell is the geographical center of the cell outline. These cells resemble the behavior of cells in culture upon a uniform increase in EGF concentration and may be responding to a uniform concentration of serum components such as EGF. Scale bar = 25 um.

Sequence 5: Host cells can be visualized as shadows as they move over a fluorescent background of tumor cells. In this sequence a large population of host granulocytes are observed moving out of blood vessels (dashed lines) onto the surface of tumor cells. Host cells are seen as dark outlines and their amoeboid movement and complete shapes are readily visualized. Areas with granulocytes are indicated by the small arrows. The cells are moving at a velocity of about 8 microns per minute but in random directions and do not appear to be chemotactic toward blood vessels. Individual tumor cells can be seen over blood vessels and as cords of tumor cells in the surrounding tissue (large arrows). The sequence repeats. 300x real time.

(7)

Conclusions

Through the use of this model, we have observed the locomotion of metastatic cells and cell surface features of these movements in live animals. It is clear that metastatic tumor cells are actively motile as they disseminate from their primary site. This information supports the three step hypothesis of metastasis (7), which purports that motility is necessary for a cell to metastasize. This model will be useful in describing and tracking the behavior and interactions of these metastatic tumor cells *in vivo*. In addition, it represents an opportunity to reliably procure pure populations of motile tumor cells in vivo under direct visualization. These cells can be used as a microbiopsy to examine gene expression patterns unique to the motile and potentially metastatic population of cells in the primary tumor. This subpopulation can be compared with adjacent but distinct populations of cells in the same tissue field by using Laser Capture Microdissection (LCM) (8, 9). Both methods of procurement of pure cell populations will allow quantitative analyses using methods based on polymerase chain reaction (PCR), reverse transcriptase-PCR, chromosome-mapping and radioimmunoassay. This would define, for the first time, how these cells differ from their non-motile neighbors in the same tumor or cells in non-metastatic tumors at the level of gene and protein composition and expression. Such analyses will lead to the discovery of genes associated with the motility phenotype in invasive and metastatic tumors which may have diagnostic and prognostic value. One can only guess at this time if such information would lead to therapeutics.

(8)

References

1. Farina, K.L., Wyckoff, J.B., Rivera, J., Lee, H., Segall, J.E., Condeelis, J.S., Jones, J.G. (1998) Cell motility of tumor cells visualized in living intact primary tumors using green fluorescent protein. *Cancer Research* 58:2528-2532. See Addendum J.

2. Neri, H., Welch, D., Kawaguchi, T. and Nicolson, G. (1982) Development and biologic properties of malignant cell sublines and clones of a spontaneously metastasizing rat mammary adenocarcinoma. *J. Natl. Cancer Inst.* 68:507-517.

3. Edmonds, B.T., Wyckoff, J., Yeung, Y.G., Wang, Y., Stanley, E.R., Jones, J., Segall, J., Condeelis, J. (1996) Elongation factor-1α is an overexpressed actin binding protein in metastatic rat mammary adenocarcinoma. *J. Cell Sci.* 109:2705-2714. See Addendum J.

4. Shestakova, Wyckoff, J., Jones, J., Singer, R., and Condeelis, J. (1998) Correlation of beta-actin mRNA localization with metastatic potential in rat adenocarcinoma cell lines. *Cancer Research.* Submitted.

5. Bailly, M., Yan, L., Whitesides, G.M., Condeelis, J.S., Segall, J.S (1998) Regulation of protrusion shape and adhesion to the substratum during chemotactic responses of mammalian carcinoma cells. *Exp. Cell Res.* In press. See Addendum J.

6. Soll (1995) The use of computers in understanding how cells crawl. *Int. Rev. Cytol.* 163:43-104.

7. Stettler-Stevenson, Aznavoorian and Liotta (1993) Tumor cell interactions with the extracellular matrix during invasion and metastasis. *Ann. Rev. Cell Biol.* 9:541-573.

8. Simone, N.L., Gillespie, J.W., Bonner, R.F., Emmert-Buck, M.R., Liotta, L.A. (1998) Laser capture microdissection: opening the microscopic frontier to molecular analysis. *Trends in Genetics* In press.

9. Emmert-Buck, M.R., Bonner, R.F., Smith, P.D., Chuaqui, R.F., Zhuang, Z. Goldstein, S.R., Weiss, R.A., Liotta, L.A. (1996) Laser capture microdissection. *Science* 274:998-1001.

(9)

Appendix

Figure Captions

Figure 1. Appearance of tumor cells in vivo and in situ. Mammary tumors were prepared by injection of GFP-expressing MTC cells (A) or MTLn3 cells (B) into the mammary fat pad of rats and imaged after 2.5 weeks of growth as described previously (2). Identical tumors were imaged from H and E stained paraffin sections as MTC (C) and MTLn3 (D) tumors. Note that MTC cells have more polarized epithelial pattern in primary tumors in contrast to MTLn3 cells. Bar, 20 uM.

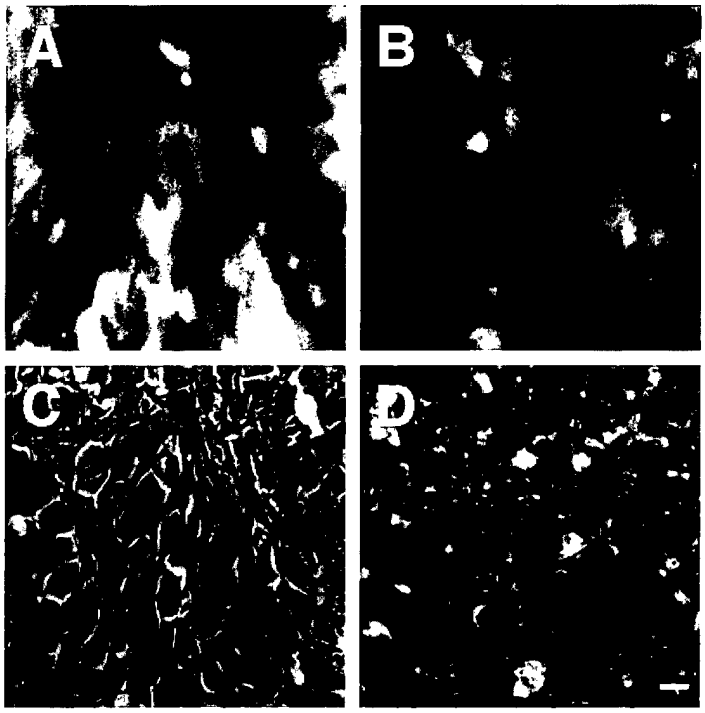
A
B
C
D

[CANCER RESEARCH 58, 2528–2532, June 15, 1998]

Advances in Brief

Cell Motility of Tumor Cells Visualized in Living Intact Primary Tumors Using Green Fluorescent Protein[1]

Kim L. Farina, Jeffrey B. Wyckoff, Johanna Rivera,[2] Herbert Lee, Jeffrey E. Segall, John S. Condeelis,[3] and Joan G. Jones

Departments of Anatomy and Structural Biology [K. L. F., J. B. W., J. R., H. L., J. E. S., J. S. C.] and Pathology [J. G. J.], Albert Einstein College of Medicine, Bronx, New York 10461

Abstract

Metastasis is the leading cause of death in cancer patients. Cell motility is believed to be a necessary step in the metastatic process (L. Liotta and W. G. Stetler-Stevenson, *In:* Cancer: Principles and Practice of Oncology, pp. 134–149, 1993). Currently, most methods available to study the behavior of metastatic tumor cells are indirect, *e.g.*, cell motility is examined *in vitro* and the results are correlated with metastatic capability (A. W. Partin, *et al.*, Cancer Treat. Res., *59:* 121–130, 1992). We have developed a model that directly examines the motility of metastatic primary tumor cells *in situ*. A metastatic rat breast cancer cell line was established that constitutively expresses green fluorescent protein. Upon s.c. injection of these cells into the mammary fat pad of female Fischer 344 rats, primary and metastatic tumors form that fluoresce when they are excited with FITC-filtered light. Animations of metastatic tumor cells moving in live rats were generated by intravital imaging of the primary tumor *in situ* on a laser scanning confocal microscope. With this model, the behavioral phenotype of metastatic and nonmetastatic tumor cells can be described and determined. This information will allow the effects of genetic manipulations or therapeutic treatments on this phenotype to be determined (D. R. Soll, Int. Rev. Cytol., *163:* 43–104, 1995). This is the first time that living primary tumor cells in a live animal have been visualized as part of a clinically relevant model.

Introduction

Metastasis is a multistep process that, for some types of tumors, is believed to require cell motility for tumor cells to invade and exit host tissues and vasculatures. Wood (1), in his pioneering studies, observed apparent *in vivo* movement of tumor cells following injection of V2 carcinoma cells into the rabbit ear vasculature. Videomicroscopy showed tumor cell extravasation, and pathology documented viable secondary metastatic implants.

Subsequent studies, noting that tumor cells are heterogeneous in their motility characteristics, focused on the potential relationship between the degree of motility and metastatic potential. Using time lapse videomicroscopy, Hosaka *et al.* (2) found that those rat hepatoma cell lines known to show early vascular invasion showed greater active locomotion *in vitro* than did those which did not. A later series of experiments by Raz *et al.* (3), which examined the behavior of closely related cell lines and clones originally derived from the same parental tumor, similarly found that highly metastatic cells show considerably more motility *in vitro* than do their low metastatic counterparts.

Studies with an emphasis on morphology have shown that tumor cells exhibit leukocyte-like motility and, more specifically, pseudopod extension. Hosaka *et al.* (4) observed movement analogous to leukocytic diapedesis in AH66F and Yoshida sarcoma cells in culture. Locker *et al.* (5), after inoculating Yoshida ascites hepatoma cells into chick embryos, documented pseudopod extension by ultrastructural examination of the resultant liver metastases in fixed tissue. Such pseudopods were even observed to be located between hepatocytes, suggesting ameboid movement. On the basis of similar observations but using an *in vitro* model system, Mohler and co-workers (6, 7) developed a visual grading system of tumor cells grown in culture, designed to predict a tumor's metastatic potential. Cumulative scores of morphological characteristics such as membrane ruffling, pseudopod extension, and vectoral translocation allowed these investigators to successfully distinguish highly metastatic cell lines from those with low metastatic potential, despite histological resemblances (8). In sum, these studies highlight the importance of motility as a positive predictor for the development of metastases. A limitation is that all of these live cell observations have been made *in vitro*.

Examples of intravital imaging systems include videomicroscopy of the microvasculature in the chorioallantoic membrane (9), the cremaster muscle, and the liver (10). In principle, the systems are similar. Fluorescently labeled tumor cells are injected into the regional vasculature and cells are observed as they lodge, extravasate, and begin to multiply. These models have substantively contributed to our knowledge of the later steps in the metastatic cascade. They give us no information, however, about how tumor cells exit their native environment, and in some cases, they are highly artificial, *e.g.*, observing the behavior of murine melanoma cells after injection into immune-deficient chick embryos.

The *in vivo* reality is that the metastatic cascade is influenced both by intrinsic properties of the tumor cell and by interactions with the host environment. It is generally agreed that, for animal models to have human clinical relevance, the model must simulate, as closely as possible, the natural biological state. Heterologous systems, for example, or models involving tumors grown in ectopic sites (xenograft models) do not permit the usual tumor-stroma interaction, which may affect both tumorigenesis and the development of metastatic subclones. Furthermore, models that use the nude mouse lack the usual host immunomodulatory mechanisms, which may also affect both the primary tumor development and its pattern of spread.

An ideal model, then, for the observation of motile events in metastasis, would be homologous, immune competent, and *in vivo*. In addition, a tracking mechanism would be needed so that tumor cells might be distinguished from normal host cells. Fluorescent labeling is possible, but this is a temporary phenomenon, restricted to one cell

Received 2/12/98; accepted 4/29/98.

The costs of publication of this article were defrayed in part by the payment of page charges. This article must therefore be hereby marked *advertisement* in accordance with 18 U.S.C. Section 1734 solely to indicate this fact.

[1] This work was supported by grants from the NIH and the Department of Defense Army Breast Cancer Program. The data in this paper will be submitted in partial fulfillment of the requirement for the Degree of Doctor of Philosophy in the Sue Golding Graduate Division of Medical Sciences, Albert Einstein College of Medicine, Yeshiva University, New York, NY (K. L. F.).

[2] Present address: Department of Medicine/Infectious Diseases, Albert Einstein College of Medicine, 1300 Morris Park Avenue, Bronx, NY 10461.

[3] To whom requests for reprints should be addressed, at Albert Einstein College of Medicine, 1300 Morris Park Avenue, Bronx, NY 10461. Phone: (718) 430-4068; Fax: (718) 430-8996; E-mail: condeeli@aecom.yu.edu.

cycle. Transfection of tumor cells with GFP[4] cDNA, however, produces a heritable, stable volume marker that allows cells to be followed long term without additional manipulations. To date, GFP has been used only in static observations of tumor cells *in vivo* or in culture conditions (11).

Here, we report a model that allows the early motile events of metastasis to be visualized at a cellular level using GFP-expressing tumor cells in live immune-competent rats. The system is homologous and uses rat mammary adenocarcinoma cells that are orthotopically injected into the mammary fat pad of female rats.

Materials and Methods

Stable Transfection. The LipofectAMINE (Life Technologies, Inc.) method was used for transfections according to the manufacturer's protocol. Cells were transfected with 11.4 μg of the pGreenLantern-1 vector (Life Technologies, Inc.) and 1.4 μg of the pSV7neo vector. Cells were assayed for GFP fluorescence 24 h after the start of the transfection. Forty-eight h after transfection, cells were placed in medium containing 0.8 mg/ml Geneticin disulfate salt (Sigma Chemical Co.).

Spectral Assays. MTLn3 and MTLn3+GFP cells were grown to 60–80% confluency, harvested with trypsin-EDTA (Life Technologies, Inc.), and resuspended in lysis buffer (0.5% Triton X-100-PBS) at a density of 1×10^6 cells/ml. The intensities of fluorescence at passages 13, 20, and 28 were determined on a Hitachi F-2000 fluorescence spectrophotometer at peak GFP excitation and emission wavelengths (489 and 512 nm, respectively).

Histopathology. To produce primary tumors, we adhered to the protocol described by Neri *et al.* (16). Briefly, s.c. injection of MTLn3 cells into the mammary fat pad of these rats results in primary tumor formation, followed by subsequent metastasis to the lymph nodes and lungs. At the time of sacrifice, the primary tumor was excised and groin and axillae were explored bilaterally for lymph nodes. Any grossly identifiable adenopathy was removed and submitted for histological examination. The abdominal, thoracic, and cranial cavities were also explored, and the lungs, liver, and brain were routinely sampled.

Intravital Imaging. For intravital imaging, the animals were anesthetized by isoflurane inhalation. The primary tumor was surgically exposed, creating a skin flap that allowed the tumor to be viewed while an intact blood supply from the superficial branch of the femoral artery was maintained (13). For viewing the tumor *in vivo,* an acrylic platform with a coverslip window was designed (Fig. 1, *bottom*). The platform rested on the microscope stage with the coverslip over the objective. The animal lay to the side of the coverslip window while the skin flap was extended from the animal. The tumor lay directly on the coverslip. This apparatus allowed animals to be maintained in a live state for several hours, facilitating extended viewing times.

Microscopy. Intravital imaging was carried out on a Bio-Rad MRC 600 CLSM system and a Nikon Diaphot inverted microscope. The system used an unattenuated Kr/Ar laser, a confocal slit of 8 mm, and an FITC filter block (laser line at 488 nm, long-pass emission filter at 515 nm). All digital images were saved using COMOS software (Bio-Rad). For time lapse imaging, single optical sections were obtained at 2-min intervals for a period of 1 h. Saved images were transferred to a Macintosh Quadra 840AV computer. Each image was processed with either Adobe Photoshop 3.0.5 or NIH Image software and viewed as an animation.

Motion Analysis. Motion analysis was performed on animations using 2D-DIAS software (Solltech, Iowa City, IA). Cell perimeters were manually traced and digitized at each time point. Centroid (cell center) location at each time point was computed from X and Y coordinates of the pixels at the perimeter of the digitized cell image. Difference pictures were generated by superimposing successive frames. The central difference method described by Maron (14) was used to determine instantaneous "velocity" (μm/min). Directional change was calculated as the absolute difference in centroid location between two consecutive frames. For velocity measurements *in vitro*, cells were videorecorded as they moved randomly on a surface or as they were subjected to a gradient of EGF delivered using a micropipette, as described elsewhere (15).

Results and Discussion

The highly metastatic MTLn3 cell line, derived from the 13762NF rat mammary adenocarcinoma, was cotransfected with the pGreenLantern-1 vector (Life Technologies, Inc.), which contains the cDNA for a humanized S65T mutant of GFP, and the pSV7neo vector. One clone, MTLn3+GFP, was chosen for its ability to retain both a fluorescent phenotype and resistance to neomycin in culture. The growth rate and morphology of the MTLn3+GFP cells were the same as those of parental MTLn3 cells. The transfected cells appear uniformly fluorescent, and the cell perimeters were easily defined. The fluorescence level of the MTLn3+GFP cells, measured by fluorescence spectrophotometry, remained stable through 30 passages in culture. This was verified by measuring the fluorescence intensity of MTLn3+GFP cell lysates, at various culture passage numbers, on a fluorescence spectrophotometer.

The metastatic involvement of tissues from rats injected with MTLn3 cells was summarized previously by Neri *et al.* (16) and Edmonds *et al.* (17). The pattern of involvement seen in this model is closely correlated with that seen clinically in breast cancer patients (18). An extensive histopathological examination was performed to establish that, upon inoculation, MTLn3+GFP cells would follow the same pattern of metastatic tissue involvement as did the parental MTLn3 cells. The results of this study indicate that the MTLn3+GFP cells retain the same metastatic phenotype displayed by parental MTLn3 cells (Table 1). Immunohistochemistry with an anti-GFP polyclonal antibody (Clontech) was performed on paraffin sections of MTLn3+GFP primary tumors. The results showed GFP expression to be homogeneous throughout all primary tumors and stable through 5 weeks postinjection (data not shown). Control MTLn3 tumors showed no positive staining for GFP.

Primary tumors and tissues with secondary involvement were dissected and viewed with light passed through an FITC filter set. We found that the primary tumor is brightly fluorescent (Fig. 1*A*, *top*). Primary tumors and their blood vessels are easily identifiable: the tumors themselves appear much brighter than the background of host tissue. This fluorescence could also be seen in metastatic tumors of the lymph nodes (data not shown) and lungs (Fig. 1*B*, *top*). The fluorescent phenotype of the MTLn3+GFP cells persisted in primary tumors and metastases throughout the life span of the animals injected. On the basis of these results, we analyzed the motility of fluorescent MTLn3 cells in primary tumors growing in live animals.

All intravital imaging, that is, imaging of an intact primary tumor in a live animal (Fig. 1, *C–E*, *top*; Figs. 2 and 3) was carried out on the laser scanning confocal microscope (Bio-Rad MRC 600) using a whole-animal platform, as shown in Fig. 1 (*bottom*). In images of regions containing both primary tumor and blood vessels, the blood vessels appear black because they are not fluorescent. The observation of blood flowing freely in the tumor's vasculature was readily observed in the microscope by eye during the imaging session (data not shown), indicating that the blood supply to the tissue was not disrupted.

To determine the characteristics of cell motility *in vivo,* time lapse imaging was performed on the tumor shown in Fig. 1, *D* and *E*, *top*. Fig. 2*A* (*arrows*) shows the single cell in Fig. 1, *D* and *E*, *top*, after displaying the time-lapse video as a series of difference pictures, rendered from DIAS software, as described in "Materials and Methods." The DIAS images demonstrate that the cell exhibits random motility with frequent changes in direction as indicated by its velocity vector (Fig. 2*A*). It is apparent from this series of images that cell perimeters are easily defined with this technology. This allows iden-

[4] The abbreviations used are: GFP, green fluorescent protein; EGF, epidermal growth factor.

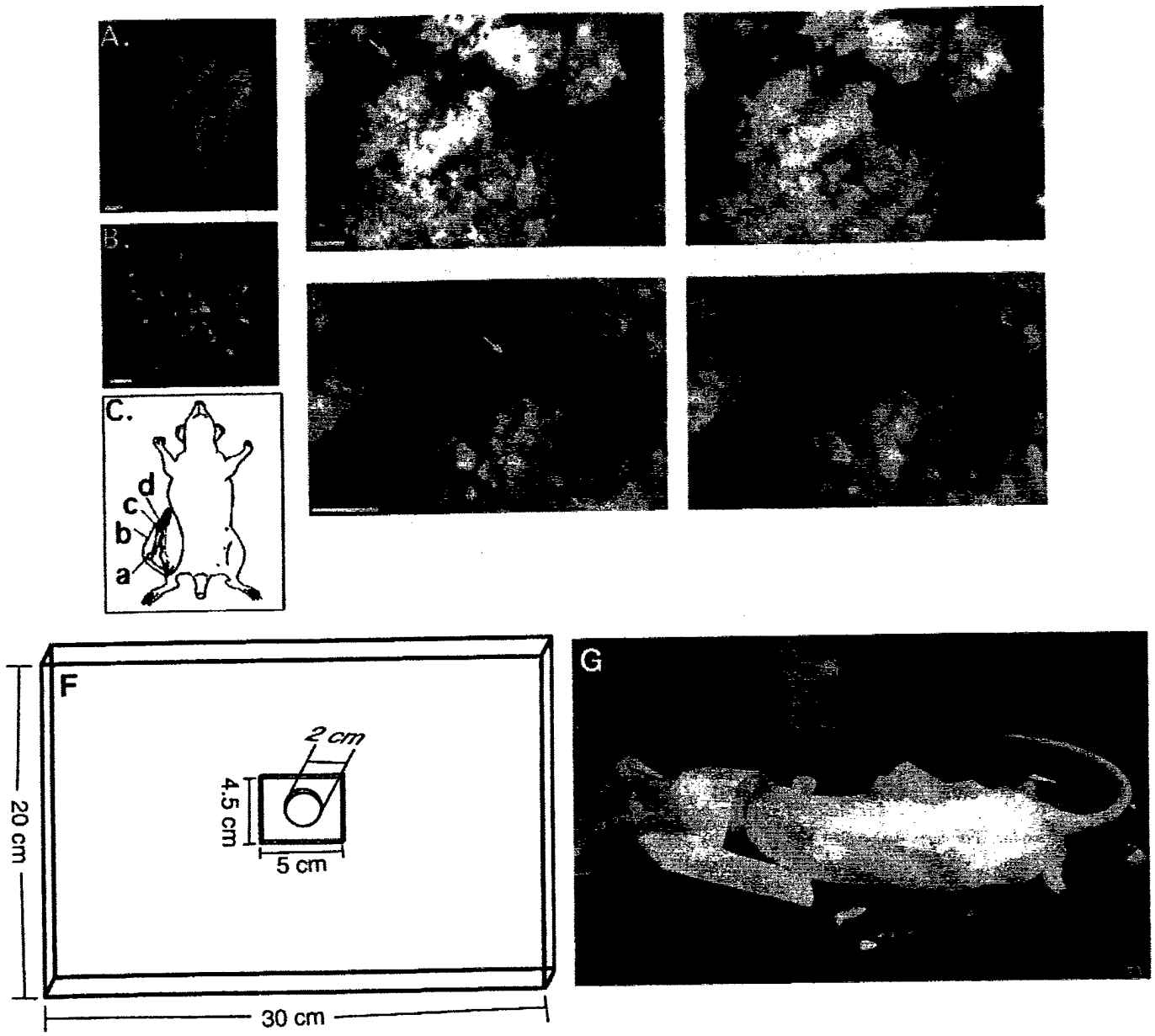

Fig. 1. Description of the GFP cell model for intravital imaging. *A–E*, fluorescent primary and metastatic lung tumors from MTLn3+GFP cells. *A*, fluorescent MTLn3+GFP cell-induced primary tumor viewed on a Zeiss Axiophot microscope. Magnification, ×1.5. This fluorescent tumor was dissected 2 weeks after injection of 1.5×10^6 cells into the mammary fat pad. For viewing this and other dissected tissues, animals were sacrificed in a CO_2 chamber. All dissected tissue was kept alive by maintenance in ice-cold PBS and viewed immediately. *Scale bar*, 1 mm. *B*, projection of lung metastasis in lung dissected four weeks after injection. This image was taken on the Bio-Rad MRC 600 scanning laser confocal microscope equipped with a ×20 dry objective (Apochromat; Nikon; numerical aperture = 0.5). To generate this image, consecutive focal planes were imaged using a Z-axis stepping motor. The image shown is a projection of the Z-series constructed by COMOS software using a maximum algorithm. *Scale bar*, 50 μm. *C*, primary tumors are exposed by minimal surgery. The primary tumor was produced according to the method of Neri *et al.* (16). The tumor was surgically exposed in the anesthetized animal creating a skin flap that allows the tumor to be viewed while an intact blood supply to the tumor and surrounding tissues was maintained. Shown in figure are: primary tumor (*a*), skin flap (*b*), superficial epigastric branch of the femoral artery (*c*), lateral thoracic artery (*d*; 13). *D* and *E*, paired stereo projections of primary tumor cells bordering a blood vessel. *Black regions* are blood vessels running through the primary tumor. *Arrow*, cell shown in Fig. 2*A*. The microscope was equipped with either a ×10 dry objective (Apochromat; Nikon; NA = 0.3; as in *D*) or a ×20 dry objective (Apochromat; Nikon; NA = 0.5; as in *E*). These stereo projections were generated as described in Fig. 1 legend. *Scale bars*, 100 μm. *F* and *G*, details of the microscope chamber used to view primary tumors in live rats. *F*: the viewing chamber was constructed from clear acrylic 0.5 cm thick with a central rectangular hole. A glass coverslip (0.15) was glued over the hole and the animal was placed face down on the viewing platform with the tumor positioned over the hole. When imaging at high magnification greater mechanical stability was achieved by placing a 2 mm thick insert into the viewing platform with a 2-cm hole in the center. The glass coverslip was then glued over the smaller hole and the tumor was positioned over the hole. This arrangement prevented bending of the glass coverslip by the weight of the animal which might disturb fine focusing with higher magnification objectives. *G*, orientation of the anesthetized animal on the viewing platform of the inverted microscope is shown.

tification of changes in cell shape over time, including extensions and retractions of pseudopods, observations that are crucial to descriptions of cell motility.

Fig. 2*B* consists of three still frames extracted from a video time-lapse obtained during imaging of an intact primary tumor in a live animal. The directed protrusion of the marked cell is clearly demonstrated as it makes its way into the field of view over a 6-min time period. The DIAS difference pictures of the same cell from the time interval $t = 10$–16 min, of a 60-min viewing period, is shown in Fig. 2*C*. In this figure, pseudopod extension occurs at the same pole of the cell at each time point, indicating successive cell movements in the same general direction. This is distinct from the type of cell movement seen in Fig. 2*A*, in which the cell remains stationary while it extends and retracts pseudopods in all directions.

Photobleaching of fluorophores is a common drawback of laser scanning confocal microscopy; it can lead to dramatic misinterpreta-

Table 1 *Metastatic involvement of tissues from rats inoculated with MTLn3 or MTLn3+GFP cells*

The timing and appearance of MTLn3+GFP cell-induced primary tumors and metastases correspond to the pattern displayed by MTLn3 parental cells. Female 49-day-old Fischer 344 rats (Charles River Laboratories) were injected s.c. with 1.0×10^6 cells (either MTLn3 or MTLn3+GFP) suspended in 150 μl of PBS under the right abdominal nipple in the region of the mammary fat pad. Tumor growth was allowed to progress for 1.5–5 weeks. Each animal was palpated and grossly inspected for metastases. In addition, primary tumors, lymph nodes, lungs, liver, and brain were excised and submitted for routine histological examination. In no cases were metastases found in the brain or liver.

	MTLn3				MTLn3+GFP			
Week	PT[a]	IPN	CLN	Lung	PT	IPN	CLN	Lung
1.5	2/3	0/3	0/3	0/3	2/3	0/3	0/3	0/3
2	3/3	1/3	0/3	0/3	3/3	0/3	0/3	0/3
3	3/3	3/3	0/3	2/3	3/3	2/3	0/3	1/3
4	3/3	3/3	0/3	3/3	3/3	3/3	0/3	2/3
5	3/3	3/3	1/3	2/3	3/3	3/3	0/3	2/3

[a] PT, primary tumor; IPN, ipsilateral lymph node; CLN, contralateral lymph node.

tion of results. In our model system, a 30% decrease in pixel intensity was calculated after obtaining eight images every 2 min over the course of 1 h. This did not affect our analyses because this level of photobleaching did not prevent identification of cell margins.

Furthermore, a more direct assessment of the effect of prolonged exposure to laser illumination was carried out on MTLn3+GFP cells by video time-lapse recording cells that were subjected to unattenuated laser confocal imaging *in vitro* while undergoing both random motility and stimulated motility in response to EGF. In both cases, the cells responded normally, as compared to the behavior of parental Mtln3 cells when exposed to low levels of white light as usually used in phase contrast imaging (15). It is important to note that no detectable changes in cell behavior were observed in the MTLn3+GFP cells, although the laser illumination used *in vitro* was more intense than that occurring *in vivo* due to light scattering caused by the presence of host tissue. For these reasons, we conclude that the cells remain fully functional and motile during laser illumination of the intact tumor.

Cellular locomotion was observed repeatedly in several experiments. The average instantaneous velocity of seven cells, from four different primary tumors, was measured as 3.0 ± 2.2 μm/min. However, in all of the tumors examined, it was apparent that only a small fraction of primary tumor cells are actively motile. One of these motile cells is shown, in Fig. 3*A*, as it moves across the field. Fig. 3*B* demonstrates the centroid and perimeter plots of the cell tracked in Fig. 3*A* (*arrows*). From these plots, an instantaneous velocity of 3.4 ± 1.5 μm/min and a persistence value of 1.48 ± 1.2 μm/min·degree was calculated. Persistence is a parameter that can be useful as an index of chemotaxis or directed cell movement (19). The persistence value demonstrated by this cell is high, taking into account the maximum (3.4 μm/min·degree) and minimum (0.07 μm/min·degree) values of persistence possible for a cell moving at a velocity of 3.4 μm/min: persistence = speed/[1 + (100/360) × directional change (in degrees)][/deq]. The velocities shown by these cells in the primary tumor are higher than velocities observed by these cells in culture during either random motility (0.45 ± 0.08, $n = 8$) or highly persistent motility (0.82 ± 0.19, $n = 8$) observed in a gradient of EGF, which is chemotactic for MTLn3 cells (15). Besides velocity and persistence, additional parameters that one can compute using a DIAS analysis are described elsewhere (19).

Through the use of this model, we have observed the locomotion of metastatic primary tumor cells and surface features of these movements in live animals. It is clear that these tumor cells are actively motile as they disseminate from their primary site. This information

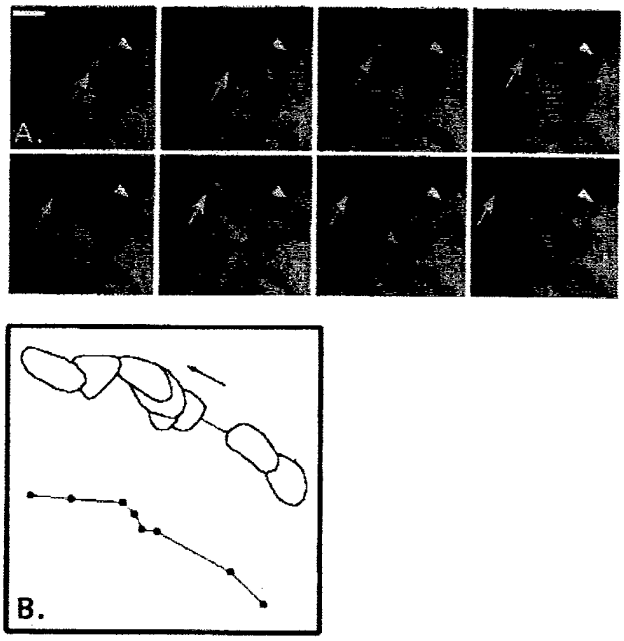

Fig. 3. Locomotion of a primary tumor cell. *A*, motile primary tumor cells observed in an intact primary tumor 2.5 weeks postinjection. Time lapse imaging was performed by obtaining single optical sections that were scanned eight times and Kalman averaged at each time point. *Arrows* follow a single cell through $t = 20$–34 min of a 60-min imaging session. *Arrowhead*, the main tumor mass; it remains stationary while the cell translocates. *Scale bar*, 50 μm. *B*, DIAS analysis of motile primary tumor cell. The path followed by the cell tracked in *A* presented as a cell perimeter plot and a centroid plot.

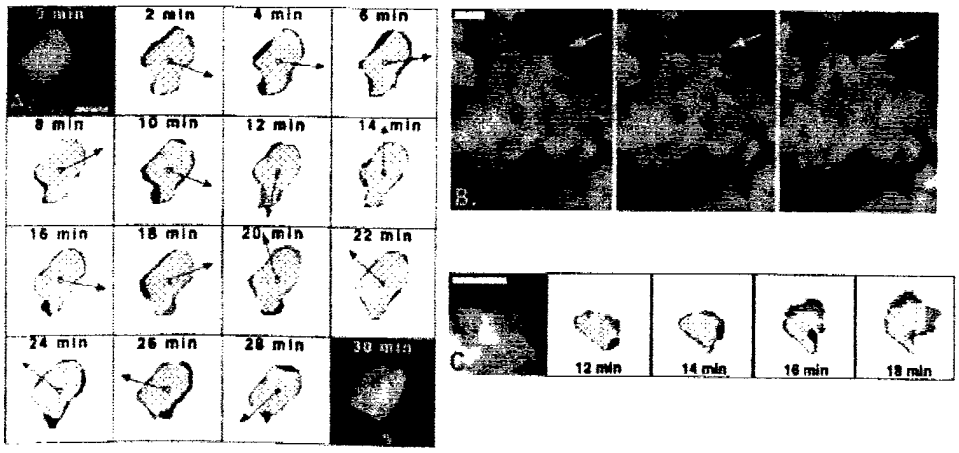

Fig. 2. DIAS analysis of a single cell of a primary tumor. *A*, shape change and random motility as shown by a single primary tumor cell. Difference analysis was performed on animations with the 2D-DIAS program (Solltech, Iowa City, IA). *Arrows*, directions of cell centroid translocation between earlier and later images. *Gray regions*, protrusive areas; *black regions*, retracted areas; *hatched regions*, common zones. *Scale bar*, 25 μm. *B*, primary tumor cell showing protrusive activity during intravital imaging. Three images from the time lapse represent a 6-min time period. *Arrows*, at the same coordinates in each frame. Note the increased protrusion of the tumor toward the *arrowhead* in each panel as time progresses. *Scale bar*, 25 μm. *C*, DIAS analysis of protrusive area shown in Fig. 2*B*. The active region of the tumor from $t = 10$–16 min, of a 60-min imaging session, was traced and analyzed with 2D-DIAS software to produce difference images, as described in *A*. *Left*, enlarged fluorescent version of the relevant area in *B* and corresponds to $t = 8$ min. *Scale bar*, 25 μm.

supports the three-step hypothesis of metastasis (20), which purports that motility is necessary for a cell to metastasize. This model will be useful not only in describing and tracking the behavior and interactions of these metastatic tumor cells *in vivo* but also in assessing the effects that genetic manipulations of key cytoskeletal proteins impart on cell motility and metastasis (19). This model will allow the direct correlation of key metastatic markers with the subpopulation of locomoting cells in a metastatic primary tumor. Additionally, it will provide a means to evaluate the impacts of treatment modalities such as pharmaceuticals, radiation, and chemotherapy on metastatic tumor cell behavior *in vivo*. It is the first model that allows direct observations of metastasis in an intact orthotopically grown primary tumor while in a live animal.

We expect that further modifications can improve the resolution of this model. Increased intensity of fluorescence can be achieved by transfection of tumor cells with new genetically enhanced versions of GFP that have increased emission and expression (12, 21, 22). We have already successfully acquired Z-series during time lapse imaging to generate three-dimensional views of cell movement (data not shown). New confocal technology with more sensitive detectors, higher light throughput, and higher speeds of image acquisition will significantly increase the spatial and temporal resolution of this type of cell imaging in intact tissue. In addition, the application of two photon confocal microscopy will allow repeated imaging of the same field without photobleaching or toxicity.

Acknowledgments

We gratefully acknowledge the staff of the Analytic Imaging Facility at Albert Einstein College of Medicine for help with imaging and Dr. Glenn Fishman for kindly providing the pSV7neo plasmid.

References

1. Wood, S. Pathogenesis of metastasis formation observed *in vivo* in the rabbit ear chamber. Arch. Pathol., *66:* 550–568, 1958.
2. Hosaka, S., Suzuki, M., and Sato, H. Leukocyte-like motility of cancer cells, with references to the mechanism of extravasation in metastasis. Gann, *70:* 559–561, 1979.
3. Raz, A., and Ben-Ze'ev, A. Cell-contact and architecture of malignant cells and their relationship to metastasis. Cancer Metastasis Rev., *6:* 3–21, 1987.
4. Hosaka, S., Suzuki, M., Goto, M., and Sato, H. Motility of rat ascites hepatoma cells, with reference to malignant characteristics in cancer metastasis. Gann, *69:* 273–276, 1978.
5. Locker, J., Goldblatt, P. J., and Leighton, J. Ultrastructural features of invasion in chick embryo liver metastasis of Yoshida ascites hepatoma. Cancer Res., *30:* 1632–1644, 1970.
6. Partin, A. W., Mohler, J. L., and Coffey, D. S. Cell motility as an index of metastatic ability in prostate cancers. Cancer Treat. Res., *59:* 121–130, 1992.
7. Mohler, J. L., Partin, A. W., Isaacs, W. B., and Coffey, D. S. Time lapse videomicroscopic identification of Dunning R-3327 prostatic adenocarcinoma and normal rate prostate cells. J. Urol., *137:* 544–547, 1987.
8. Mohler J. L., Partin, A. W., and Coffey, D. S. Prediction of metastatic potential by a new grading system of cell motility: validation in the Dunning R-3327 prostatic adenocarcinoma model. J. Urol., *138:* 168–170, 1987.
9. MacDonald, I. C., Schmidt, E. E., Morris, V. L., Chambers, A. F., and Groom, A. C. Intravital videomicroscopy of the chorioallantoic microcirculation. Microvasc. Res., *44:* 185–199, 1992.
10. Morris, V. L., MacDonald, I. C., Koop, S., Schmidt, E. E., Chambers, A. F., and Groom, A. C. Early interactions of cancer cells with the microvasculature in mouse liver and muscle during hematogenous metastasis: videomicroscopic analysis. Clin. Exp. Metastasis, *11:* 377–390, 1993.
11. Chishima, T., Miyagi, Y., Wang, X., Yamaoka, H., Shimada, H., Moossa, A. R., and Hoffman, R. M. Cancer invasion and micrometastasis visualized in live tissue by green fluorescent protein expression. Cancer Res., *57:* 2042–2047, 1997.
12. Yang, T-T., Cheng, L., and Kain, S. R. Optimized codon usage and chromophore mutations provide enhanced sensitivity with the green fluorescent protein. Nucleic Acids Res., *22:* 4592–4593, 1996.
13. Petry, J. J. The anatomy of the epigastric flap in the experimental rat. Plast. Reconstr. Surg., *74:* 410–413, 1984.
14. Maron, M. J. Numerical Analysis. New York: Macmillan Publishing Co., 1982.
15. Bailly, M., Yan, L., Whitesides, G., Condeelis, J., and Segall, J. Regulation of protrusion shape and adhesion to the substratum during chemotactic responses of mammalian carcinoma cells. Exp. Cell Res., in press, 1998.
16. Neri, A., Welch, D., Kawaguchi, T., and Nicolson, G. L. Development and biologic properties of malignant cell sublines and clones of a spontaneously metastasizing rat mammary adenocarcinoma. J. Natl. Cancer Inst. (Bethesda), *68:* 507–517, 1982.
17. Edmonds, B. T., Wyckoff, J., Yeung, Y. G., Wang, Y., Stanley, E. R., Jones, J., Segall, J., and Condeelis, J. Elongation factor-1α is an overexpressed actin binding protein in metastatic rat mammary adenocarcinoma. J. Cell Sci., *109:* 2705–2714, 1996.
18. Haagensen, C. D. The natural history of breast cancer. *In:* C. D. Haagensen (ed.), Diseases of the Breast, Ed. 3, pp. 635–718. Philadelphia: W. B. Saunders Co., 1986.
19. Soll, D. R. The use of computers in understanding how animal cells crawl. Int. Rev. Cytol., *163:* 43–104, 1995.
20. Liotta, L. A., and Stetler-Stevenson, W. G. Principles of molecular cell biology of cancer: cancer metastasis. *In:* V. T. DeVita, Jr., S. Hellman, and S. A. Rosenberg (eds.), Cancer: Principles and Practice of Oncology, Ed. 4, pp. 134–149. Philadelphia: J. B. Lippincott Co., 1993.
21. Zhang, G., Gurtu, V., and Kain, S. R. An enhanced green fluorescent protein allows sensitive detection of gene transfer in mammalian cells. Biochem. Biophys. Res. Commun., *227:* 707–711, 1996.
22. Kimata, Y., Iwaki, M., Lim, C. R., and Kohno, K. A novel mutation which enhances the fluorescence of green fluorescent protein at high temperatures. Biochem. Biophys. Res. Commun., *232:* 69–73, 1997.

(11)

Bibliography

Papers

1. Farina, K.L., Wyckoff, J.B., Rivera, J., Lee, H., Segall, J.E., Condeelis, J.S., and Jones, J. (1998) Cell motility of tumor cells visualized in living intact primary tumors using green fluorescent protein. *Cancer Research* 58, 2528-2532.

2. Bailly, M., Yan, L., Whitesides, G.M., Condeelis, J.S., Segall, J.E. (1998) Regulation of protrusion shape and adhesion to the substratum during chemotactic responses of mammalian carcinoma cells. *Exp. Cell Res.* 241, 285-299.

3. Wyckoff, J.B., Insel, L., Khazaie, K., Lichtner, R.B., Condeelis, J., and Segall, J.E. (1998) Suppression of ruffling by the EGF receptor in chemotactic cells. *Experimental Cell Research* 242, 100-109.

Abstracts

Condeelis, J., Chan, A., Farina, K., Bailly, M., Jones, J., and Segall, J. (1998) EGF-receptor-stimulated chemotaxis in breast adenocarcinoma cells: Molecular mechanisms relating to protrusion, adhesion and protein synthesis. Motility and Metastasis Keystone Symposium. February 21-26, 1998. (Liotta, Kohn and Zetter, Org.).

Farina, K.L., Wyckoff, J.B., Rivera, J., Lee, H., Segall, J.E., Condeelis, J.S., and Jones, J. (1998) Cell motility visualized in living intact primary tumors using green fluorescent protein. Motility and Metastasis Keystone Symposium. February 21-26, 1998. (Liotta, Kohn and Zetter, Org.).

Bailly, M., Chan, A., Segall, J. and Condeelis, J. (1998) Ultrastructural definition of the polymerization zone induced at the leading edge of metastatic carcinoma cells after EGF stimulation. Motility and Metastasis Keystone Symposium. February 21-26, 1998. (Liotta, Kohn and Zetter, Org.).

List of all personnel:

Dr. John Condeelis, Principal Investigator

Mr. Jeffrey B. Wyckoff, Research Technician C